Supporting Information

Wang et al. 10.1073/pnas.1716322115

SI Materials and Methods

Reagents, Antibodies, and Plasmids. Chemicals were purchased from Sigma-Aldrich unless otherwise indicated. DL-AP5 (0105), CNQX (0190), and BMI (0130) were purchased from Tocris Bioscience. Information on primary antibodies is as follows: mouse anti-GluA1 [MAB2263, 1:1,000 for Western blot (WB); Millipore]; mouse anti-GluA2 (MAB397, 1:1,000 for WB; Millipore); mouse anti-GluN1 (114011, 1:1,000 for WB; Synaptic Systems); rabbit anti-GluN2A (PPS012; 1:1,000 for WB; R&D Systems); mouse anti-GluN2B [75–097, 1:1,000 for WB; Developmental Studies Hybridoma Bank (DSHB)]; rabbit anti-Flag (F7425, 1:2,000 for WB; Sigma); mouse anti-PSD95 (MAB1598, 1:1,000 for WB; Millipore); mouse anti-syntaxin1 (SC12736, 1:1,000 for WB; 1:50 for co-IP; Santa Cruz); mouse anti-SNAP25 (SC20038, 1:50 for co-IP; Santa Cruz); rabbit anti-SNAP25 (ab5666, 1:2,000 for WB; Abcam); mouse anti-VAMP2 (MAB5136, 1:2,000 for WB; R&D Systems); mouse anti-synaptotagmin1 (mAB30, 1:50 for WB; DSHB); mouse anti-synaptophysin [#5461, 1:1,000 for WB; Cell Signaling Technology (CST)]; rabbit anti-RIM1α (140003, 1:1,000 for WB; Synaptic Systems); rabbit anti-Complexin1/2 (122022, 1:2,000 for WB; Synaptic Systems); mouse anti–Munc13-1 (126111, 1:1,000 for WB; Synaptic Systems); rabbit anti–Munc18-1 (116002, 1:1,000 for WB; Synaptic Systems); mouse anti-Nrg3 (SC390171, 1:1,000 for WB; Santa Cruz); rabbit anti-GFAP (Z0334, 1:5,000 for WB; DAKO); rabbit anti-Tuj1 (ab18207, 1:2,000 for WB; Abcam); rabbit anti-ErbB4 (0618, 1:2,000 for WB, from Cary Lai, Indiana University, Bloomington, IN); rabbit anti–phospho-ErbB4 (#4757, 1:1,000 for WB; CST); mouse anti-Myc (#2276, 1:2,000 for WB; 1:500 for co-IP; CST); rabbit anti-V5 (#13202, 1:2,000 for WB; CST); mouse anti–β-actin (MABT523, 1:5,000 for WB; Millipore); mouse anti-NeuN (MO22122; 1:1,000 for staining; Neuromics). Horseradish peroxidase-conjugated secondary antibodies were purchased from Thermo Fisher Scientific (31460 for goat anti-rabbit, 31430 for goat anti-mouse). The cDNA of *Nrg3* was generated by PCR and subcloned into p3×Flag-CMV. The cDNA of SNAP25, syntaxin1 (syntaxin1A), and VAMP2 was generated by PCR and subcloned into pcDNA 3.1/myc-His with a stop code before the myc-his tag. Truncations of syntaxin1 were all generated by PCR and subcloned into pRK5 with a Myc-tag in the N terminus. SYT1-V5 (HsCD00439877), Munc18-1-V5 (HsCD00445098), and Complexin1-V5 (HsCD00440711) were purchased from DNASU Plasmid Repository. The authenticity of all constructs was verified by DNA sequencing and Western blot analysis.

Animals. Mice were housed in a room at 24 °C in a 12-h light/dark cycle with access to food and water ad libitum. $Nrg3^{f/f}$ mice were generated by flanking exon 2 of the *Nrg3* gene with loxP sites. PCR-based genotyping was performed on genomic DNA isolated from the tail or cortex. $Nrg3^{f/f}$ mice were genotyped with a forward primer (TGG ACT TCA GCG AGA GAC AC) and a reverse primer (CTT CTC CTT CCC AGC TCT AG). The two primers amplified 230 bp from the wild-type *Nrg3* allele or 345 bp from the floxed Nrg3 allele. $Nrg3^{f/f}$ (C57BL) mice were crossed with GFAP-Cre transgenic mice (1) to produce $GFAP\text{-}Nrg3^{f/f}$ mice. *GFAP-Cre* mice were genotyped with a forward primer (ACT CCT TCA TAA AGC CCT) and a reverse primer (ATC ACT CGT TGC ATC GAC CG), which generate a PCR product of 190 bp. $Nrg3^{f/f}$ mice were crossed with Nex-Cre mice (2) to produce $Nex\text{-}Nrg3^{f/f}$ mice. *Nex-Cre* mice were genotyped with primer 1 (GAG TCC TGG AAT CAG TCT TTT TC), primer 2 (ATC ACT CGT TGC ATC GAC CG), and primer 3 (CCG CAT AAC CAG TGA AAC AG). Primers 1 and 2 amplify a 770-bp product from the wild-type Nex allele and primers 1 and 3 amplify a 525-bp fragment from the Nex-Cre allele. Male mice were used in all biochemical experiments, electrophysiology recordings, and behavioral tests. Experimental procedures were approved by the Institutional Animal Care and Use Committee of Augusta University.

Cell Cultures and Transfection. HEK293T cells were cultured in DMEM (10–013; Corning Cellgro) supplemented with 10% FBS (100–106; Gemini Bio Products). Transient transfection was performed using polyethylenimine (408727; Sigma), as described before (3). In brief, cells in a 60-mm dish (at ∼70% cell confluence) were incubated with precipitates formed by 5 μg of plasmid DNA with 220 μL of polyethylenimine 0.05% (wt/vol). Thirty-six hours after transfection, cells were lysed in the lysis buffer (50 mM Tris·HCl, pH 7.4, 150 mM NaCl, 1% Nonidet P-40, 0.5% Triton X-100) plus protease inhibitors and centrifuged at 16,000 × *g* at 4 °C for 10 min. The supernatant was collected and measured for protein concentration using the bicinchoninic acid (BCA) protein assay kit (23225; Pierce) and subjected to co-IP.

Lentivirus Production. Lentivirus was prepared as described previously (4). Flag-Nrg3 was generated by PCR and subcloned into the pFUGW vector (kindly provided by Hongjun Song, University of Pennsylvania, Philadelphia). pFUGW-Flag-Nrg3, pCMV△8.92, and pVSVG were cotransfected into HEK293T cells by calcium phosphate precipitation. Flag-Nrg3 was driven by the human ubiquitin C promoter. Lentivirus was harvested 48 h after transfection and concentrated to a final 10^8 infection units/mL.

Western Blotting. Western blotting was performed as described previously (3). Brain tissues were homogenized in RIPA buffer (50 mM Tris·HCl, pH 7.4, 150 mM NaCl, 2 mM EDTA) containing 0.5% sodium deoxycholate, 0.1% SDS, 1 mM PMSF, 1 mM Na_3VO_4, 1 mM NaF, 1 mM DTT, and protease inhibitor mixture. Samples were centrifuged at 12,000 × *g* for 20 min at 4 °C to remove debris. Lysates (∼50 μg of protein) were resolved by SDS/PAGE and transferred to PVDF membrane (ISEQ00010; Millipore). The membrane was immunoblotted with antibodies, and immunoreactive bands were visualized by enhanced chemiluminescence (32106; Pierce). Film was scanned and quantitated by using NIH ImageJ 1.42q.

Neuron Culture. Hippocampal neurons were cultured as described previously (5) with modifications. Briefly, hippocampi were isolated, kept separate from one another in cold HBSS (14175; Gibco), and incubated with 20 units/mL of papain (LK003178; Worthington) at 37 °C for 15 min. Dissociated cells were suspended in plating media (DMEM supplemented with 10% FBS) and plated at a density of 6×10^4 per well onto poly-L-lysine–coated 18-mm coverslips (12–545-100; Fisherbrand) in 12-well plates (130185; Thermo Fisher Scientific). Cells were incubated for 4 h before replacing the medium with the maintenance medium containing Neurobasal medium (21103–049; Gibco) supplemented with 2% B-27 supplement (17504–044; Gibco), 1% GlutaMax (35050–061; Gibco), and 1% penicillin/streptomycin (15140–122; Gibco). Neurons were maintained at 37 °C in 5% CO_2, with half of the medium changed every 2–3 d with the maintenance medium. Neurons were infected with lentiviruses expressing GFP or Flag-Nrg3 at 20 multiplicities 4 d before experiments. Infection efficiency was monitored by GFP expression. Neurons from a >90% infection were subjected to electrophysiological recording.

Immunostaining. Immunostaining was performed as described previously (6). Briefly, mice were deeply anesthetized with isoflurane

and perfused with PBS followed by ~30 mL 4% paraformaldehyde (PFA) until bodies became stiff. Brains were postfixed in 4% PFA at 4 °C overnight and dehydrated using 30% sucrose at 4 °C for 2 d. Brain tissues were embedded in optimal cutting temperature compound (4583; Tissue-Tek), rapidly frozen, and cut into 40-μm sections. Sections were blocked and permeabilized in PBS containing 0.3% Triton X-100 and 5% goat serum for 2 h at room temperature. Sections were incubated at 4 °C overnight with primary antibodies in PBS containing 5% goat serum and 2% BSA. Sections were washed with PBS, incubated at room temperature for 1 h with Alexa 594-conjugated goat anti-mouse IgG (A11005; Molecular Probes), and mounted using ProLong Gold Antifade Reagent with DAPI (P36931; Molecular Probes).

Subcellular Fractionation. Hippocampal subcellular fractions were prepared as described previously with modifications (7). All procedures were performed at 4 °C, and buffers or solutions contained protease inhibitors and phosphatase inhibitors (50 mM NaF, 1 mM sodium orthovanadate, 20 mM β-glycerophosphate). Briefly, brain tissues were homogenized in 10 vol of the Hepes-buffered sucrose (0.32 M sucrose, 4 mM Hepes/NaOH, pH 7.4) with a glass-Teflon homogenizer. Homogenates were centrifuged at 1,000 × *g* for 10 min to remove nuclear and other cell debris to collect the supernatant (S1). S1 fraction was centrifuged at 10,000 × *g* for 15 min to obtain the crude synaptosomal fraction (P2) and supernatant (S2). The P2 pellet was resuspended in water for hypoosmotic shock for <10 s, which was rapidly adjusted to 4 mM Hepes and incubated on a rotator at 4 °C for 30 min. The resuspended P2 was centrifuged at 25,000 × *g* for 20 min to yield the supernatant (S3, crude synaptic vesicle fraction) and pellet (P3, synaptosomal membrane fraction). The S3 fraction was centrifuged at 160,000 × *g* at 4 °C for 60 min to yield the pellet that was enriched with synaptic vesicle protein (SV fraction). The P3 pellet was resuspended in the Hepes-buffered sucrose, carefully layered on top of a discontinuous gradient containing 0.8, 1.0, and 1.2 M sucrose (top to bottom), and centrifuged at 150,000 × *g* at 4 °C for 2 h. The gradient yielded a floating myelin fraction (G1, the top layer), a light membrane fraction at the 0.8 M/1.0 M sucrose interface (G2), and a synaptosomal plasma membrane fraction at the 1.0 M/1.2 M sucrose interface (G3). The G3 fraction was incubated with 1% Triton X-100 in 50 mM Hepes/NaOH (pH 8.0) at 4 °C for 30 min and subjected to centrifugation at 25,000 × *g* for 1 h to yield the supernatant (presynaptic membrane fraction) and the pellet (postsynaptic membrane fraction).

Co-IP. The supernatant of HEK293T cell lysates and presynaptic fractions was precleared by incubating at 4 °C for 1 h with protein A/G PLUS-Agarose beads (SC2003; Santa Cruz). Precleared samples were incubated with respective antibodies overnight at 4 °C. Mouse IgG (SC2025; Santa Cruz) was used as a negative control. The immune complexes were incubated with protein A/G PLUS-Agarose beads for 4 h at 4 °C. Beads were washed four times with lysis buffer before being suspended with an equal volume of 2× SDS sample buffer. For Flag-tagged proteins, the supernatant was incubated with anti-Flag M2 affinity gel (A2220; Sigma) for precipitation.

Analysis of the SNARE Complex. Biochemical analysis of the SNARE complex was performed as previously described with modifications (8). HEK293T cells were cotransfected with pCDNA-syntaxin1, VAMP2, and SNAP25 (1:1:1) together with or without Flag-Nrg3. In some experiments, HEK293T cells were cotransfected with pCDNA-syntaxin1, VAMP2, SNAP25, SYT1-V5, Munc18-1-V5, and Complexin1-V5 (1:1:1:1:1:1) together with or without Flag-Nrg3. Total DNA was kept constant by balancing a Nrg3 plasmid with an empty plasmid. Thirty-six hours after transfection, cells were homogenized with the lysis buffer (50 mM Tris·HCl, pH 7.4, 150 mM NaCl, 1% Nonidet P-40, 0.5% Triton X-100) plus protease inhibitors and centrifuged at 16,000 × *g* at 4 °C for 10 min. The supernatant was mixed with SDS-sample butter and divided into two fractions. One fraction was boiled for 20 min and the other was not. Both fractions were subjected to SDS/PAGE and Western blot analysis. SDS-resistant SNARE complexes were defined as the immunoreactive material above 40 kDa that was absent from boiled samples.

Electrophysiological Recording. Hippocampal slices were prepared as described previously (9). Brains were isolated from anesthetized mice (5–7 wk old, male) and chilled in ice-cold modified artificial cerebrospinal fluid (ACSF) containing (in mM): 220 glycerol, 2 KCl, 10 $MgSO_4$, 0.2 $CaCl_2$, 1.3 NaH_2PO_4, 26 $NaHCO_3$, and 10 glucose. Coronal hippocampal slices (300 μm) were cut in ice-cold modified ACSF using a VT-1000S vibratome (Leica) and incubated in regular ACSF containing (in mM) (126 NaCl, 3 KCl, 1 $MgSO_4$, 2 $CaCl_2$, 1.25 NaH_2PO_4, 26 $NaHCO_3$, and 10 glucose) at 32 °C for 30 min and at room temperature (25 ± 1 °C) for an additional hour. Slices were placed in the recording chamber, which was superfused (2 mL/min) with ACSF at 32–34 °C. CA1 pyramidal neurons were visualized with infrared optics using an upright microscope with a 40× water-immersion lens (Axioskop 2 Plus; Zeiss) and infrared-sensitive CCD camera (C2400-75; Hamamatsu) and recorded with glass pipettes, which were pulled by a micropipette puller (P-97, Sutter Instrument) with a resistance of 3–5 MΩ. Data were acquired by a MultiClamp 700B amplifier and a 1440A digitizer (Molecular Device). For some co-IP experiments, hippocampal slices were incubated in a high-K^+ solution (in mM) (79 NaCl, 70 KCl, 1 $MgSO_4$, 2 $CaCl_2$, 1.25 NaH_2PO_4, 26 NaHCO3, and 10 glucose, a corresponding decrease of NaCl to maintain isoosmolarity) for 10 min to depolarize.

For sEPSC recording, pyramidal neurons were clamped at −70 mV in the presence of 20 μM BMI with the pipette solution containing (in mM): 125 Cs-methanesulfonate, 5 CsCl, 10 Hepes, 0.2 EGTA, 1 $MgCl_2$, 4 Mg-ATP, 0.3 Na-GTP, 10 phosphocreatine, and 5 QX314 (pH 7.40, 285–300 mOsm). In some experiments, transfected neurons were recorded with bath solution containing (in mM): 140 NaCl, 5 KCl, 1 $MgSO_4$, 2 $CaCl_2$, 1.25 NaH_2PO_4, 26 $NaHCO_3$, and 10 glucose (pH 7.4, 285–300 mOsm). sIPSCs were recorded at −70 mV in the presence of 20 μM CNQX and 100 μM DL-AP5, with the pipette solution containing (in mM): 140 CsCl, 10 Hepes, 0.2 EGTA, 1 $MgCl_2$, 4 Mg-ATP, 0.3 Na-GTP, 10 phosphocreatine, and 5 QX314 (pH 7.40, 285–300 mOsm). In some experiments, before recording, hippocampal slices were incubated with 5 μM PD158780 (2615; Tocris Bioscience), an inhibitor of ErbB4 (10, 11).

The electric property of CA1 excitatory neurons was characterized in a current-clamped configuration, in response to a series of depolarizing pulses (from 50 to 120 pA at a step of 10 pA) in the presence of 20 μM CNQX, 100 μM DL-AP5, and 20 μM BMI. The pipette solution contained (in mM): 125 K-gluconate, 5 KCl, 10 Hepes, 0.2 EGTA, 1 $MgCl_2$, 4 Mg-ATP, 0.3 Na-GTP and 10 phosphocreatine (pH 7.40, 285 mOsm). Membrane input resistance was calculated in response to a series of hyperpolarizing pulses. For paired-pulse ratio recording, EPSCs were evoked by stimulating the SC-CA1 pathway at a holding potential of −70 mV in the presence of 20 μM BMI. Intervals of paired stimulations were set at 25, 50, and 100 ms. Ratios were defined as [(p2/p1)] × 100, where p1 and p2 are the amplitudes of EPSCs evoked by the first and second pulse, respectively.

For the MK-801 block assay, CA1 pyramidal neurons were clamped at +40 mV. Evoked NMDAR-mediated EPSCs were recorded in response to 0.1 Hz of presynaptic stimulation in the presence of 20 μM CNQX and 20 μM BMI. Slices were treated with 40 μM MK801 for 5 min before evoking and recording EPSCs for 20 min. EPSC amplitudes were normalized to the first EPSC and fitted with single-exponential functions to calculate decay constants (τ, number of stimuli). For the minimal stimulation recording, CA1 pyramidal neurons were clamped at −70 mV. EPSCs were evoked by stimulating the SC-CA1 pathway (0.067 Hz)

with ACSF-filled glass pipettes. Stimulus intensity was adjusted to fulfill the following four criteria: (*i*) all or none synaptic events were generated; (*ii*) little or no variation in EPSC latency; (*iii*) no change in mean size or shape of EPSCs by a small change in stimulus intensity; and (*iv*) complete failure to evoke EPSCs by a 10–20% reduction in stimulus intensity. Responses that did not meet these criteria were rejected.

In all experiments, series resistance was controlled below 20 MΩ and not compensated. Cells were rejected if membrane potentials were more positive than −60 mV or if series resistance fluctuated more than 20% of initial values. All recordings were done at 32–34 °C. Data were filtered at 1 kHz and sampled at 10 kHz.

Behavioral Test. Locomotor activity, PPI, and the Y maze were measured as described previously (5). Mice were placed in a chamber (50 × 50 × 10 cm). Movement in the chamber was monitored for 30 min using an overhead camera and tracking software (EthoVision; Noldus). PPI was tested in sound-attenuated chambers (San Diego Instruments). Before the test, mice were allowed to habituate to the chamber with a 65-dB background white noise for 5 min. During the test, mice were placed in a Plexiglass tube mounted on a plastic frame to monitor motion by a piezoelectric accelerometer and subjected to 12 startle trials (120 dB, 20 ms) and 12 prepulse/startle trials (20-ms white noise at 70, 75, or 80 dB at 100-ms intervals and 20-ms 120-dB startle stimulus). Different trial types were presented pseudorandomly with each trial type presented 12 times, and no two consecutive trials were identical. Mouse movement was measured during 100 ms after startle stimulus onset (sampling frequency 1 kHz). PPI (%) was calculated according to the formula: 100 × (startle amplitude for pulse alone − startle response for pulse for prepulse)/startle amplitude for pulse alone.

For working memory, mice were subjected to a Y-maze test by being placed at the center of a Y-shaped maze with three arms represented by A, B, and C (35 cm). They were allowed to move freely through the maze for 8 min. The total number and series of arm entries were recorded. Nonoverlapping entrance sequences (e.g., ABC, BCA) were defined as spontaneous alternations. A sucrose preference test was performed as previously described (12). Briefly, mice were single-housed for 1 wk and habituated with two bottles of 1% sucrose for 3 d, which was followed by two bottles of water for 1 d. Mice were then water-deprived for 24 h and exposed to one bottle of water and one bottle of 1% sucrose for 1 h in the dark and for another 1 h after switching the bottle positions. Total consumption of each fluid was measured, and the sucrose preference was defined as the ratio of the consumption of sucrose solution versus the consumption of both water and sucrose solution during the 2-h test. Social interaction was measured in a black Plexiglas rectangular box that consisted of three interconnected chambers as previously described (13). After habituation, a mouse was allowed to explore the three chambers for 10 min. If it showed a preference for one side of the chamber, the mouse was excluded from the test. In the first phase, the mouse was placed in the center chamber with both gates to the side chambers closed. A stranger wild-type mouse (S1) was then introduced into the cage of one chamber while the other chamber had one empty cage (E), which served as an inanimate object with no social valence. After opening both gates, the test mouse was monitored for the distance to the S1 and E cages for 10 min. In the second phase, the test mouse was placed in the center chamber with both gates closed; the S1 mouse was placed in the E cage and a second stranger wild-type mouse (S2) was placed in the previous S1 cage. The test mouse was allowed to freely explore and monitored for the distance to either cage for 10 min. The time spent within 2 cm of each cage was analyzed.

Statistical Analyses. Statistical analyses were performed using Graph Pad Prism software. Two-tailed unpaired Student's *t* test was used to compare data from two groups. One-way ANOVA was used to compare data from more than two groups. Two-way ANOVA was used in behavioral and electrophysiological studies with more than two parameters; "*n*" represents the number of animals or cultures tested. Data were presented as mean ± SEM. The accepted level of significance was $P < 0.05$.

1. Zhuo L, et al. (2001) hGFAP-cre transgenic mice for manipulation of glial and neuronal function in vivo. *Genesis* 31:85–94.
2. Goebbels S, et al. (2006) Genetic targeting of principal neurons in neocortex and hippocampus of NEX-Cre mice. *Genesis* 44:611–621.
3. Tao Y, et al. (2013) Erbin interacts with TARP γ-2 for surface expression of AMPA receptors in cortical interneurons. *Nat Neurosci* 16:290–299.
4. Lu Y, et al. (2014) Maintenance of GABAergic activity by neuregulin 1-ErbB4 in amygdala for fear memory. *Neuron* 84:835–846.
5. Jiao HF, et al. (2017) Transmembrane protein 108 is required for glutamatergic transmission in dentate gyrus. *Proc Natl Acad Sci USA* 114:1177–1182.
6. Bean JC, et al. (2014) Genetic labeling reveals novel cellular targets of schizophrenia susceptibility gene: Distribution of GABA and non-GABA ErbB4-positive cells in adult mouse brain. *J Neurosci* 34:13549–13566.
7. Huang YZ, et al. (2000) Regulation of neuregulin signaling by PSD-95 interacting with ErbB4 at CNS synapses. *Neuron* 26:443–455.
8. Burré J, et al. (2010) Alpha-synuclein promotes SNARE-complex assembly in vivo and in vitro. *Science* 329:1663–1667.
9. Sun XD, et al. (2016) Lrp4 in astrocytes modulates glutamatergic transmission. *Nat Neurosci* 19:1010–1018.
10. Pitcher GM, Beggs S, Woo RS, Mei L, Salter MW (2008) ErbB4 is a suppressor of long-term potentiation in the adult hippocampus. *Neuroreport* 19:139–143.
11. Tan GH, et al. (2011) Neuregulin 1 represses limbic epileptogenesis through ErbB4 in parvalbumin-expressing interneurons. *Nat Neurosci* 15:258–266.
12. Towell A, Muscat R, Willner P (1987) Effects of pimozide on sucrose consumption and preference. *Psychopharmacology (Berl)* 92:262–264.
13. Yin DM, et al. (2013) Reversal of behavioral deficits and synaptic dysfunction in mice overexpressing neuregulin 1. *Neuron* 78:644–657.

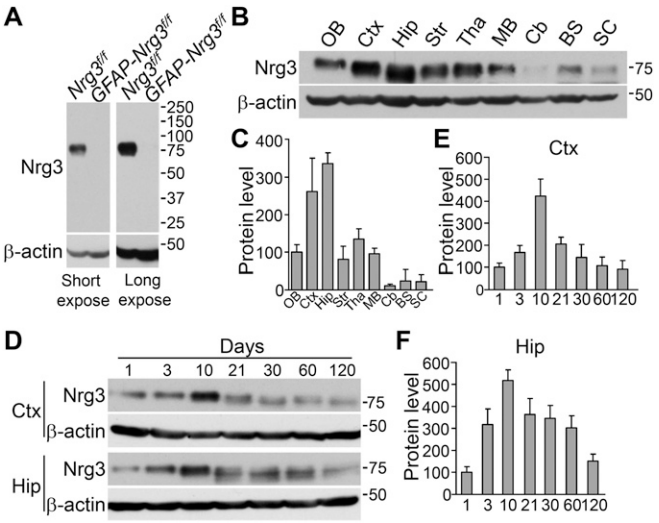

Fig. S1. Enriched expression of Nrg3 in the hippocampus and cortex. (*A*) Specificity of anti-Nrg3 antibody. Hippocampal and cortical lysates were subjected to Western blotting with anti-Nrg3 antibody. Only one band at the predicted molecular weight, ~75 kDa, was detected (*Left*), even after longer exposure (*Right*). The band was not detectable in tissues from *GFAP-Nrg3*$^{f/f}$ mice. (*B*) Nrg3 enriched in hippocampus and cortex. Different brain subregions were subjected to Western blotting, with β-actin as loading control. BS, brainstem; Cb, cerebellum; Ctx, cortex; Hip, hippocampus; MB, middle brain; OB, olfactory bulb; SC, spinal cord; Str, striatum; Tha, thalamus. (*C*) Quantitative data in *B*. The Nrg3 level in OB was designated at 100%; $n = 3$ independent experiments. (*D*) Increased Nrg3 expression in neonatal cortex and hippocampus. (*E* and *F*) Quantitative data in *D*. The Nrg3 level at P1 was designated as 100%; $n = 3$ from independent experiments.

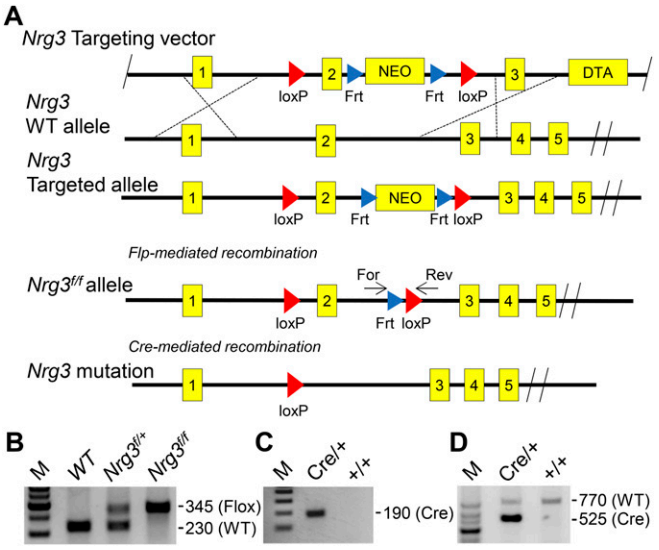

Fig. S2. Generation and characterization of Nrg3 conditional mutant mice. (*A*) Genomic structure of the Nrg3 gene and different alleles. (*B*) PCR genotyping for Nrg3 floxed mice. Wild-type and *Nrg3*$^{f/f}$ mice generated 230 bp and 345 bp, respectively. (*C* and *D*) PCR genotyping for GFAP-Cre and Nex-Cre mice.

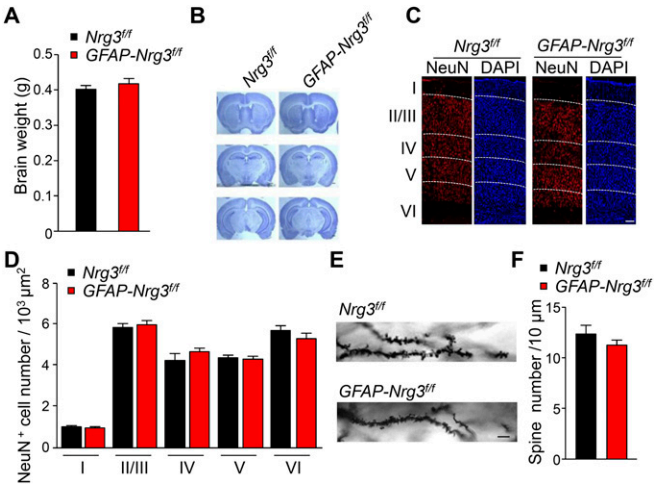

Fig. S3. Characterization of gross morphology and neuron numbers of *GFAP-Nrg3*$^{f/f}$ mice. (*A*) Similar brain weights of *Nrg3*$^{f/f}$ and *GFAP-Nrg3*$^{f/f}$ mice; n = 4 mice for each genotype; *t* test; $P > 0.05$. (*B*) Similar brain gross morphology of *Nrg3*$^{f/f}$ and *GFAP-Nrg3*$^{f/f}$ mice. Brain sections at three different positions from Bregma were subjected to Nissl staining. (*C*) Similar numbers of NeuN-expressing neurons in the somatosensory cortex of *Nrg3*$^{f/f}$ and *GFAP-Nrg3*$^{f/f}$ mice at P60. (Scale bar: 100 μm.) (*D*) Quantification of data in *C*; n = 10 slices from three mice per genotype; *t* test; $P > 0.05$. (*E*) Representative images of basal dendrites of CA1 neurons. *Nrg3*$^{f/f}$ and *GFAP-Nrg3*$^{f/f}$ mice (2 mo old) were subjected to Golgi staining. (Scale bar: 10 μm.) (*F*) Quantitative analysis of data in *E*. Data were collected from 15 neurons from three mice per genotype; *t* test; $P > 0.05$.

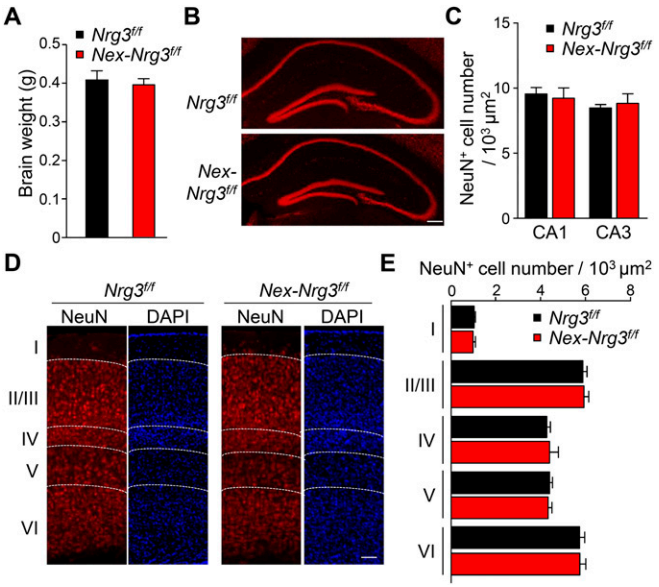

Fig. S4. Characterization of gross morphology and neuron numbers of *Nex-Nrg3*$^{f/f}$ mice. (*A*) Similar brain weights of *Nrg3*$^{f/f}$ and *Nex-Nrg3*$^{f/f}$ mice; n = 4 mice for each genotype; *t* test; $P > 0.05$. (*B*) No apparent deficits in the hippocampal structure of *Nex-Nrg3*$^{f/f}$ mice at P60. (Scale bar: 250 μm.) (*C*) Quantification of NeuN-expressing cells in hippocampal CA1 and CA3 regions; n = 10 slices from three mice per genotype; *t* test; $P > 0.05$. (*D*) No apparent deficits in the somatosensory cortex of *Nex-Nrg3*$^{f/f}$ mice at P60. (Scale bar: 50 μm.) (*E*) Quantification of NeuN-expressing neurons in the somatosensory cortex; n = 10 slices from three mice per genotype; *t* test; $P > 0.05$.

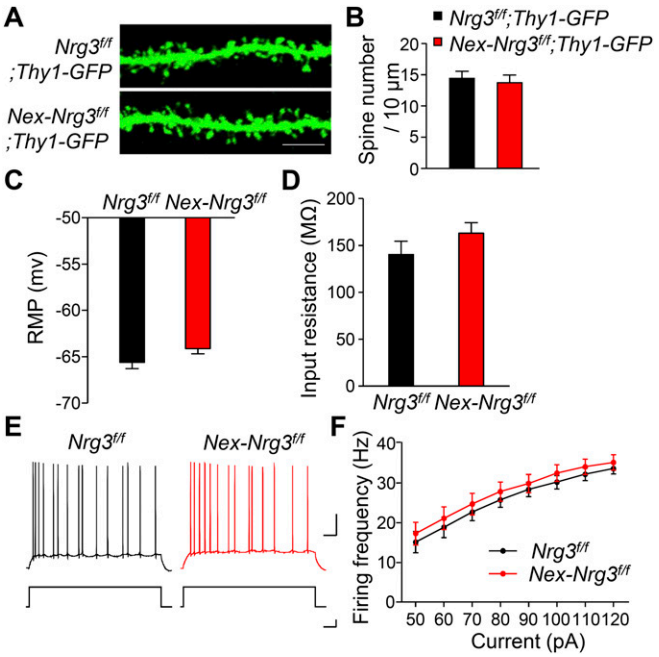

Fig. S5. Normal intrinsic property of CA1 pyramidal neurons in *Nex-Nrg3*$^{f/f}$ mice. (*A*) Representative spine images of CA1 pyramidal neurons. Hippocampal slices were prepared from 2-mo-old mice of indicated genotypes. (Scale bar: 5 μm.) (*B*) Quantitative analysis of data in *A*; $n = 3$–4 basal dendrite segments, 15 neurons from three mice per genotype; *t* test; $P > 0.05$. (*C* and *D*) Resting membrane potential (RMP) and input resistance; $n = 13$ from three mice per genotype; *t* test; $P > 0.05$. (*E*) Representative traces of spikes in CA1 pyramidal neurons. (Scale bars: *Top*, 100 ms, 20 mv; *Bottom*, 100 ms, 20 pA.) (*F*) Firing rates plotted against increasing injected currents. $n = 11$ from 3 *Nrg3*$^{f/f}$ mice and $n = 12$ from 3 *Nex-Nrg3*$^{f/f}$ mice; Two-way ANOVA; $P > 0.05$.

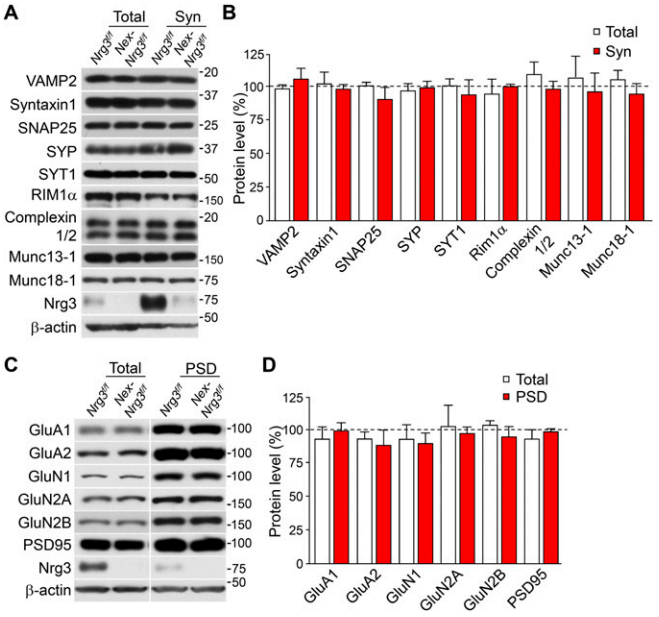

Fig. S6. Similar levels of synaptic proteins between *Nex-Nrg3*$^{f/f}$ mice and control mice. (*A*) Similar levels of presynaptic proteins in *Nex-Nrg3*$^{f/f}$ mice, compared with control mice. Homogenates (Total) and synaptosomal fraction (Syn) of the hippocampus were subjected to Western blotting. (*B*) Quantitative analysis of data in *A*; $n = 3$ per genotype; *t* test; $P > 0.05$. (*C*) Similar levels of postsynaptic proteins in *Nex-Nrg3*$^{f/f}$ mice, compared with control mice. Homogenates (Total) and PSD fraction of the hippocampus were subjected to Western blotting. (*D*) Quantitative analysis of data in *C*; $n = 3$ per genotype; *t* test; $P > 0.05$.

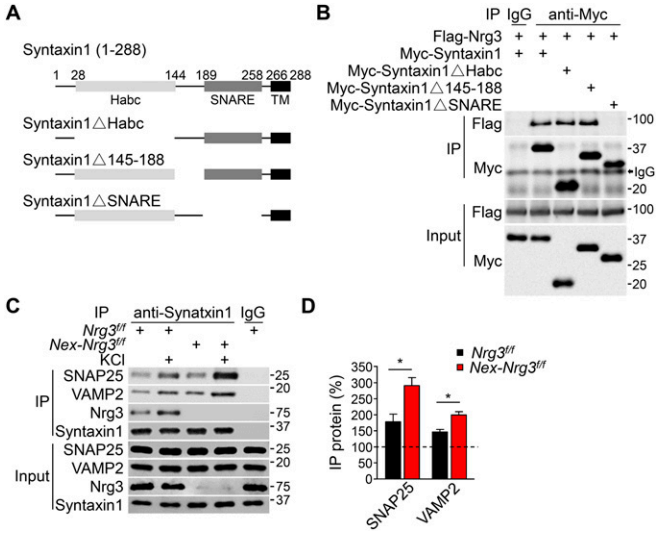

Fig. S7. Nrg3 binds to the SNARE domain of Syntaxin1 and regulates the SNARE-complex assembly. (*A*) Schematic diagrams of syntaxin1 and mutants. Numbers on the diagrams correspond to amino acid residues in syntaxin1A. Habc, the three-helical bundle Habc domain; SANRE, the SNARE domain; TM, the transmembrane domain. (*B*) The SNARE domain of syntaxin1 is required for interacting with Nrg3. Flag-Nrg3 and Myc-syntaxin1 or mutants were cotransfected in HEK293T cells. Cell lysates were immunoprecipitated with mouse anti-Myc antibody. Resulting complexes were probed for Flag and Myc. Note that Flag-Nrg3 was pulled down only by Myc-syntaxin1, Myc-syntaxin1△Habc, and Myc-syntaxin1△145–188, but not Myc-syntaxin1△SNARE. (*C*) Increased association of syntaxin1 with SNARE proteins (SNAP25 and VAMP2) in KCl-treated slices. Hippocampal brain slices were incubated with 70 mM KCl for 10 min. Lysates were incubated with mouse syntaxin1 antibody, and resulting immunoprecipitates were probed for indicated SNARE proteins. (*D*) Quantitative analysis of data in *C*. The expression of immunoprecipitated proteins with no KCl treatment were considered as 100%; $n = 3$ independent experiments; *t* test; $^*P < 0.05$.

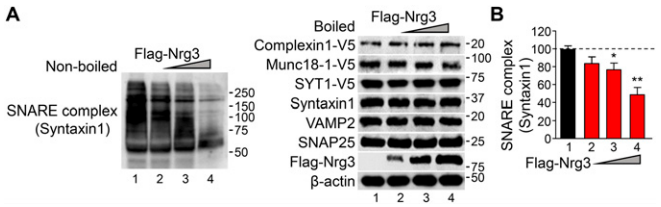

Fig. S8. Overexpression of Nrg3 inhibits SNARE-complex assembly. (*A*) A dose-dependent reduction in SNARE-complex assembly by Nrg3. HEK293T cells were cotransfected with syntaxin1, VAMP2, SNAP25, Complexin1-V5, Munc18-1-V5, and SYT1-V5 and increasing amounts of Flag-Nrg3. Cell lysates were immunoblotted without (*Left*) and with boiling (*Right*); SNARE complexes above 40 kDa were probed with antibody to syntaxin1, and the boiled samples were probed with antibodies to syntaxin1, SNAP25, VAMP2, Flag, and V5. (*B*) SNARE-complex assembly was quantitated and normalized to β-actin; $n = 3$ independent experiments; one-way ANOVA; $^*P < 0.05$; $^{**}P < 0.01$.

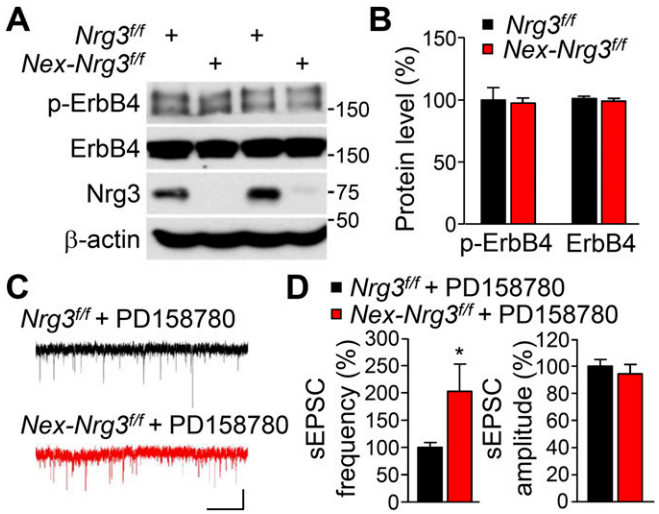

Fig. S9. sEPSC frequency in *Nex-Nrg3*$^{f/f}$ slices remained increased in the presence of PD158780, an ErbB4 inhibitor. (*A*) Similar phosphorylated ErbB4 (p-ErbB4) and ErbB4 levels in *Nrg3*$^{f/f}$ and *Nex-Nrg3*$^{f/f}$ mice. (*B*) Quantitative analysis of data in *A*; $n = 3$ per genotype; *t* test; $P > 0.05$. (*C*) Representative traces of sEPSCs in CA1 pyramidal neurons from PD158780-treated slices. (Scale bars: 2 s, 20 pA.) (*D*) Quantitative data of frequency and amplitude; $n = 8$ neurons from three mice per genotype; *t* test; $^*P < 0.05$.